Review Article | Gastrointestinal Imaging

eISSN 2005-8330
https://doi.org/10.3348/kjr.2021.0112
Korean J Radiol 2022;23(1):13-29

Korean Journal of Radiology
KJR

Quantitative Evaluation of Hepatic Steatosis Using Advanced Imaging Techniques: Focusing on New Quantitative Ultrasound Techniques

Junghoan Park[1], Jeong Min Lee[1, 2, 3], Gunwoo Lee[4], Sun Kyung Jeon[1, 2], Ijin Joo[1, 2]

[1]Department of Radiology, Seoul National University Hospital, Seoul, Korea; [2]Department of Radiology, Seoul National University College of Medicine, Seoul, Korea; [3]Institute of Radiation Medicine, Seoul National University Medical Research Center, Seoul, Korea; [4]Ultrasound R&D 2 Group, Health & Medical Equipment Business, Samsung Electronics Co., Ltd., Seoul, Korea

Nonalcoholic fatty liver disease, characterized by excessive accumulation of fat in the liver, is the most common chronic liver disease worldwide. The current standard for the detection of hepatic steatosis is liver biopsy; however, it is limited by invasiveness and sampling errors. Accordingly, MR spectroscopy and proton density fat fraction obtained with MRI have been accepted as non-invasive modalities for quantifying hepatic steatosis. Recently, various quantitative ultrasonography techniques have been developed and validated for the quantification of hepatic steatosis. These techniques measure various acoustic parameters, including attenuation coefficient, backscatter coefficient and speckle statistics, speed of sound, and shear wave elastography metrics. In this article, we introduce several representative quantitative ultrasonography techniques and their diagnostic value for the detection of hepatic steatosis.

Keywords: *Liver; Liver steatosis; Quantitative evaluation; Ultrasound imaging; Quantitative ultrasound*

INTRODUCTION

Nonalcoholic fatty liver disease (NAFLD) is a spectrum of liver abnormalities that present with excessive fat accumulation [1-3]. The prevalence of NAFLD has been steadily increasing, and it is currently the most common chronic liver disease in Western countries as well as in Asia [4-8]. Although simple fatty liver, also called nonalcoholic fatty liver (NAFL), is generally considered non-progressive, it can progress to nonalcoholic steatohepatitis (NASH) and clinically significant liver fibrosis [9]. In addition, the increased degree of hepatic steatosis in NAFLD is associated with a higher prevalence of metabolic syndrome and increased cardiovascular risk [10]. Therefore, efforts are actively being made to treat NAFLD. Hepatic steatosis in NAFLD seems to be reversible through treatment, including lifestyle interventions [11]. Furthermore, hepatic steatosis is frequently found in other chronic liver diseases, such as chronic hepatitis C, and the degree of hepatic steatosis is possibly associated with the hepatic fibrosis progression rate in a specific genotype of chronic hepatitis C [12]. Therefore, the detection and grading of hepatic steatosis are important for prognostication and management decisions for patients with NAFLD and other chronic liver diseases.

Currently, liver biopsy is considered the gold standard for the diagnosis and severity assessment of hepatic steatosis [3,13]. However, liver biopsy has intrinsic limitations of sampling errors and its invasiveness hinders its use. Accordingly, there is a need for reliable non-invasive biomarkers for the assessment of hepatic steatosis [14]. At present, MR spectroscopy (MRS) and MRI-proton density fat fraction (MRI-PDFF) have been accepted as non-invasive reference standards for quantifying hepatic steatosis [15-17]. However, these MR-based techniques

Received: February 3, 2021 **Revised:** July 26, 2021
Accepted: August 31, 2021
Corresponding author: Jeong Min Lee, MD, PhD, Department of Radiology, Seoul National University Hospital, 101 Daehak-ro, Jongno-gu, Seoul 03080, Korea.
• E-mail: jmsh@snu.ac.kr

have limitations, as they are expensive and not readily accessible. In contrast, conventional B-mode ultrasound is inexpensive and easily accessible, and it has been widely used for the assessment of hepatic steatosis in clinical settings despite its subjectivity [18]. Recently, various quantitative ultrasound (QUS) techniques that quantitatively characterize tissue microstructure using inherent ultrasound tissue properties, have been developed and actively validated for the diagnosis of hepatic steatosis [19-25].

Here, we will briefly review conventional imaging techniques for hepatic fat quantification, and discuss the basic concepts and recent advances in QUS techniques and their diagnostic performance in hepatic fat quantification. In addition, the unmet needs of the current QUS techniques and the future direction of development for the evaluation of NASH/NAFLD will be briefly discussed.

Conventional Imaging Techniques for Liver Fat Quantification

B-Mode Ultrasound

B-mode ultrasound is the most common imaging modality used to evaluate hepatic steatosis. Using B-mode ultrasound, hepatic steatosis can be graded based on the following findings: 1) higher echogenicity of the liver than that of the renal cortex, 2) impaired visualization of the intrahepatic vessels, and 3) impaired visualization of the diaphragm and posterior right hepatic lobe due to ultrasound beam attenuation (Fig. 1) [26]. Although B-mode ultrasound has the advantages of high accessibility and low cost, especially compared with MRI, it is limited by its relatively low sensitivity for detecting mild hepatic steatosis (73.3% for detection of > 0%–5% steatosis) [27] and its substantial intra- and inter-observer variability (κ = 0.54 and 0.43, respectively) [28].

CT

On unenhanced CT images, the normal liver parenchyma has a slightly higher attenuation than the spleen, whereas the hepatic attenuation value (Hounsfield unit [HU]) decreases with increasing severity of hepatic steatosis [29,30]. The generally accepted criteria for diagnosis of hepatic steatosis (hepatic fat content ≥ 30%) on unenhanced CT are as follows: 1) the absolute attenuation of the liver is less than 40 HU [31], or 2) the attenuation of the liver is at least 10 HU less than that of the spleen [32]. CT can detect hepatic steatosis with high specificity (93.5%, 88.1%, and 94.6% for diagnosis of > 0%–5%, > 10%–20% and > 25%–33% steatosis, respectively) but has a relatively low sensitivity, especially for mild cases (46.1%, 57.0%, and 72.0% for detection of > 0%–5%, > 10%–20% and > 25%–33% steatosis, respectively) [27]. Furthermore, hepatic attenuation can also be affected by other factors, including iron or glycogen deposition and drug therapy (e.g., amiodarone), which can act as confounders [33]. More importantly, exposure to ionizing radiation discourages its widespread use for the diagnosis of hepatic steatosis.

MR-Based Methods

MR-based techniques have been extensively validated as quantitative tools for hepatic steatosis [27,34,35]. At present, PDFF measured by these MR-based techniques is accepted as a noninvasive reference standard for hepatic steatosis, and may replace liver biopsy [15-17]. There are two major MR-based techniques for hepatic fat quantification: MRS and multi-echo Dixon MRI.

MR Spectroscopy (MRS)

^{1}H-MRS is based on the difference between the precession frequencies of protons in different chemical moieties (chemical shifts) [27,36,37]. To obtain MRS-PDFF of the liver, a localization voxel with dimensions of 2 x 2 x 2 cm^3 or 3 x 3 x 3 cm^3 is typically placed within the right hepatic lobe to avoid the large intrahepatic vessels and liver edge (Fig. 2A) [38]. Then, the PDFF of a target volume can be calculated by adding all the individual lipid peak areas in the MRS frequency spectrum and dividing it by the sum of the lipid and water peaks (Fig. 2B) [33,36].

Several previous studies have shown that MRS is highly accurate in diagnosing hepatic steatosis using histologic results as a reference standard (area under the receiver operating characteristic curve [AUROC], 0.97–0.99 for detection of hepatic steatosis ≥ S1) [34,35]. However, MRS has an intrinsic limitation; it allows fat quantification of a small portion, usually a single voxel, of the liver, which may lead to sampling variability. Furthermore, MRS requires technical expertise for acquisition and analysis because of its complexity, which limits its widespread use [33,39].

Multi-Echo Dixon MRI

Fat quantification using multi-echo Dixon MRI is also based on the chemical shift phenomenon between fat and water protons. In gradient echo (GRE) imaging, the signals

https://doi.org/10.3348/kjr.2021.0112

Korean Journal of Radiology
KJR

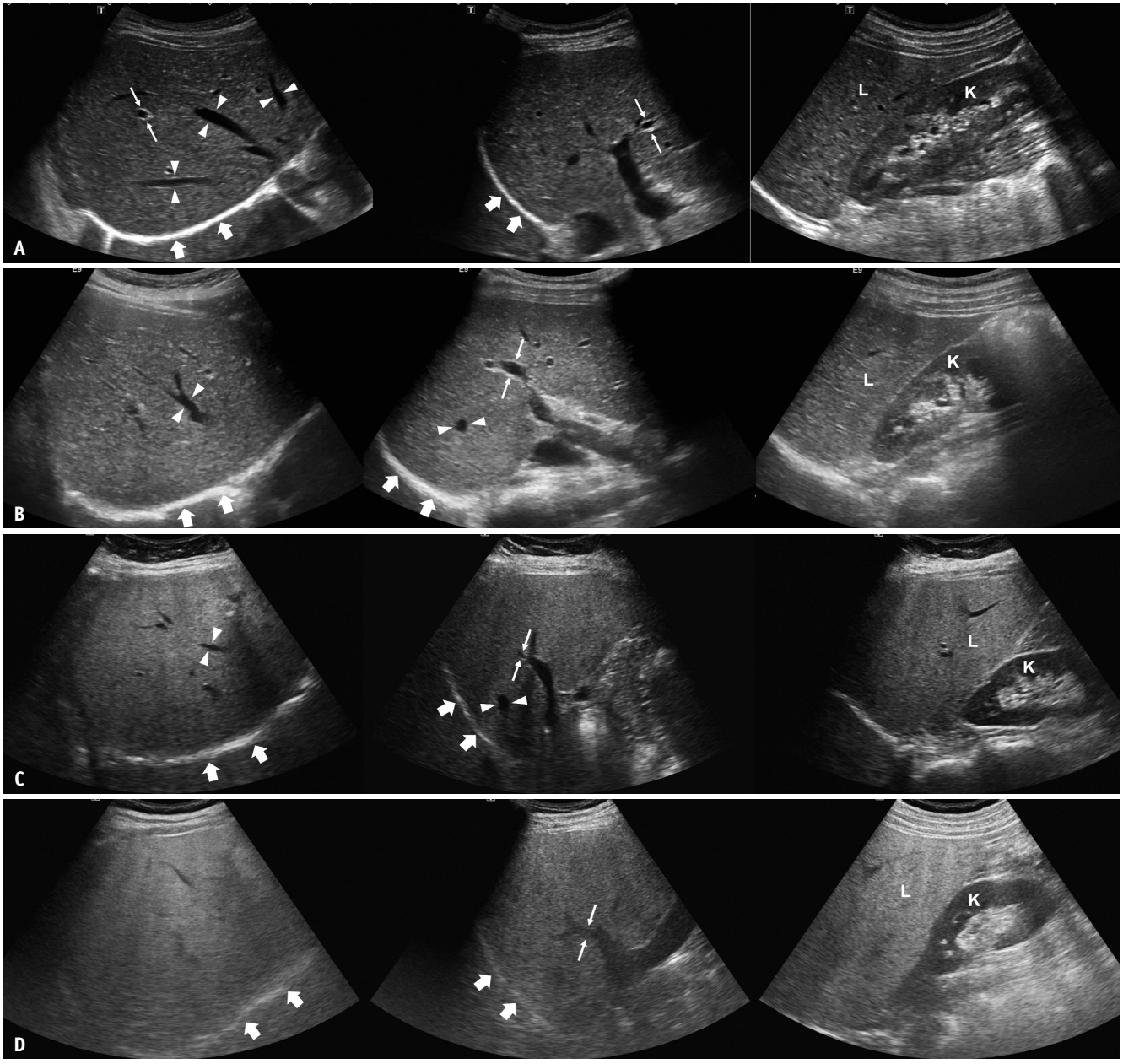

Fig. 1. Conventional ultrasound images of patients with different degrees of hepatic steatosis in subcostal view (left), intercostal view (middle), and longitudinal view with right kidney (right).
A. A 37-year-old female patient without hepatic steatosis. Echogenicity of the liver (L) is similar to that of the right kidney (K). Hepatic veins (arrowheads), wall of portal veins (thin arrows), and diaphragm (thick arrows) are all clearly visualized. **B.** A 20-year-old female patient with mild hepatic steatosis. Echogenicity of the liver (L) is higher than that of the right kidney (K). However, hepatic veins (arrowheads), wall of portal veins (thin arrows), and diaphragm (thick arrows) are all visualized. **C.** A 60-year-old female patient with moderate hepatic steatosis. Echogenicity of the liver (L) is higher than that of the right kidney (K). Hepatic veins (arrowheads) and wall of portal veins (thin arrows) are partly blurred due to ultrasound beam attenuation, but the diaphragm (thick arrows) is still visualized. **D.** A 49-year-old male patient with severe hepatic steatosis. Echogenicity of the liver (L) is markedly higher than that of the right kidney (K). The wall of the portal vein (thin arrows), as well as the diaphragm (thick arrows), are blurred due to ultrasound beam attenuation.

from fat and water periodically dephase and rephase owing to the difference between their precession frequencies [36,40]. When obtaining in-phase and out-of-phase signals, which is called a two-point Dixon method, a fat signal fraction can simply be estimated using the following equation:

 https://doi.org/10.3348/kjr.2021.0112

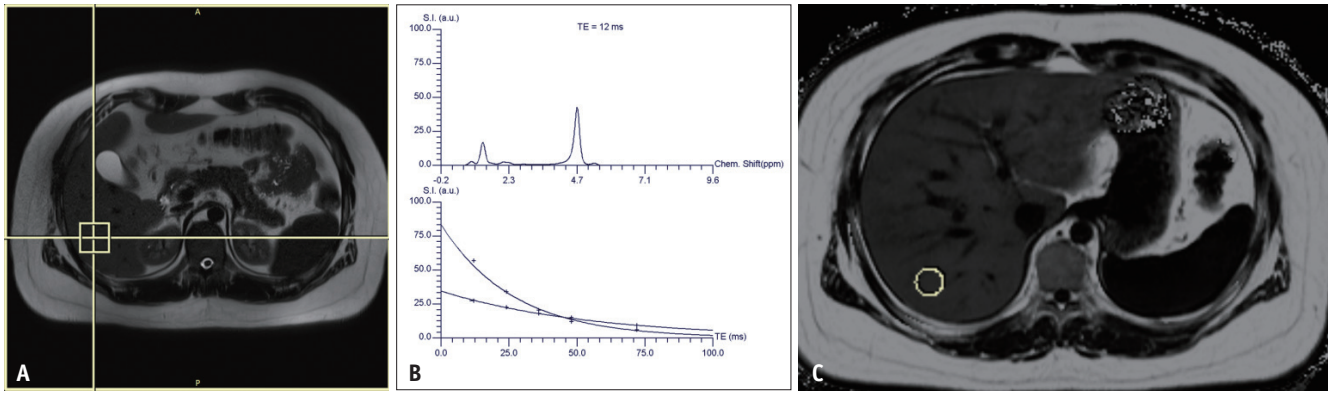

Fig. 2. MRS (A, B) and MRI-proton density fat fraction (C) results of a patient with hepatic steatosis.
A. A 3 x 3 x 3 cm-sized voxel was placed in the right hepatic lobe for MRS. **B.** The MRS frequency spectrum (upper) at the voxel shows a large water peak at 4.7 ppm as well as multiple lipid peak areas at a lower ppm. Fat and water signals at different TEs are plotted (lower), and the T2-corrected fat signal fraction is calculated by 29.3%. **C.** Fat signal fraction map acquired with multi-echo Dixon MRI in the same patient: brighter areas indicate higher fat signal fraction. A 2 cm-sized circular ROI is placed in the right hepatic lobe, and the fat signal fraction for the ROI was calculated as 24.4%. MRS = MR spectroscopy, ROI = region of interest, TE = echo time

$$S_{IP} = W + F,\ S_{OP} = W - F \text{ (if } F < W)$$

$$\therefore \text{ Fat signal fraction} = \frac{F}{W + F} = \frac{|S_{IP} - S_{OP}|}{2S_{IP}}$$

where S_{IP} and S_{OP} refer to signal intensities in the in-phase and out-of-phase images, respectively, and W and F refer to the signals from water and fat, respectively [41,42].

However, this method is limited by the dynamic range of the fat fraction from 0%–50%, and it can be affected by confounding factors, including T1 bias, T2* decay, and the spectral complexity of fat [38]. Recent multi-echo Dixon techniques have overcome these confounding factors using a low flip angle, T2* correction with multiple echoes, and multi-peak spectral modeling [38,43,44]. Using these multi-echo Dixon techniques, the signals from water and fat can be accurately separated and the fat signal fraction map of the entire liver can be obtained by calculating the signal ratio of the proton density of fat to the sum of those of fat and water (MRI-PDFF) (Fig. 2C) [38].

MRI-PDFF is highly accurate for the diagnosis and severity assessment of hepatic steatosis (AUROC, 0.98, 0.91, and 0.90 for ≥ S1, S2, and S3 in a meta-analysis, respectively) [45]. The diagnostic performance of MRI-PDFF is comparable to that of MRS (AUROC, 0.88 vs. 0.86 for ≥ S2) [46]; however, MRI-PDFF is more easily applicable because it does not require a technical expert for acquisition and analysis. MRI-PDFF has been widely used as a reference standard for performance studies on the quantification of hepatic steatosis and is the preferred endpoint for NASH clinical trials [16,17,39].

QUS Techniques

Although conventional B-mode ultrasound is used for a wide range of medical indications, quantitative information from B-mode ultrasound images is limited because ultrasound images are highly dependent on machine settings. However, recent technical developments allow ultrasound scanners not only to deliver images but also to obtain raw radiofrequency (RF) data, which enables the development of QUS [47]. QUS measures various acoustic parameters, including the attenuation coefficient (AC) [48], backscatter coefficient (BSC), speckle statistics [49,50], speed of sound [51,52], and elastography metrics [53,54] from the tissue, most of which are obtained from the raw RF data rather than processed images [47]. It aims to estimate tissue properties from these acoustic parameters by using appropriate models and theories of how ultrasound interacts with the tissue [47]. Since QUS can provide quantitative data related to tissue properties, it has been studied and utilized in various medical fields [49] such as the assessment of osteoporosis [55], characterization of the myocardium [56], characterization of breast and thyroid lesions [57-59], detection of prostate cancer and metastatic lymph nodes [60,61], and assessment of tumor response to chemotherapy [62,63], among others. In addition, QUS is expected to be effective in detecting hepatic steatosis, because the acoustic properties of hepatic tissue change with hepatic fat accumulation. Accordingly, multiple QUS techniques based on various acoustic parameters have been developed to quantitatively evaluate hepatic steatosis

https://doi.org/10.3348/kjr.2021.0112

Korean Journal of Radiology
KJR

[64]. In this article, we introduce several representative QUS techniques based on AC, BSC, and speckle statistics for the evaluation of hepatic steatosis, which are briefly summarized in Table 1 and Figure 3.

Attenuation Coefficient (AC)

Attenuation refers to the energy loss when an ultrasound wave passes through tissue, and it is dependent on the tissue properties and the ultrasound frequency [64]. Ultrasound attenuation increases with hepatic fat infiltration, which obscures the hepatic vessels and diaphragm during conventional ultrasound [65-67]. AC is a quantitative measure of energy loss during ultrasound transmission [67]. There are two major approaches for the evaluation of hepatic steatosis using AC: 1) controlled attenuation parameter (CAP) obtained with the transient elastography device, using A-mode ultrasound and 2) B-mode ultrasound-guided attenuation imaging.

Controlled Attenuation Parameter (CAP)

CAP is one of the most widely studied QUS techniques for the quantification of hepatic steatosis, which uses an ultrasound-based vibration-controlled transient elastography (VCTE™) device (Fibroscan, Echosens). CAP is assessed simultaneously with liver stiffness measurement using raw RF data acquired by FibroScan [19]. To measure CAP, a

Table 1. Summary of Quantitative Ultrasound Techniques for Evaluating Hepatic Steatosis

	Attenuation	Backscatter (Including Speckle Statistics)
Physical meaning	Energy loss as ultrasound wave passes through tissue	Scatter that occurs when ultrasound wave strikes the microstructure of tissue
Ultrasound image appearance	Hypoechoic appearance at distant field in ultrasound image	Echogenic appearance in ultrasound image
Relationship with hepatic steatosis	Increasing with fat content	Increasing with fat content
Approach	AC (dB/cm/MHz), CAP (dB/m)	BSC, speckle statistics
Available software	Attenuation measurement without liver visualization - CAP (Echosens) Attenuation imaging using B-mode ultrasound - ATI (Canon Medical Systems) - UGAP (GE Healthcare) - ATT (Hitachi) - Att PLUS (SuperSonic Imagine) - TAI (Samsung Medison)	BSC - Nothing commercialized Speckle statistics - ASQ (Canon Medical Systems) - TSI (Samsung Medison)

AC = attenuation coefficient, BSC = backscatter coefficient, CAP = controlled attenuation parameter

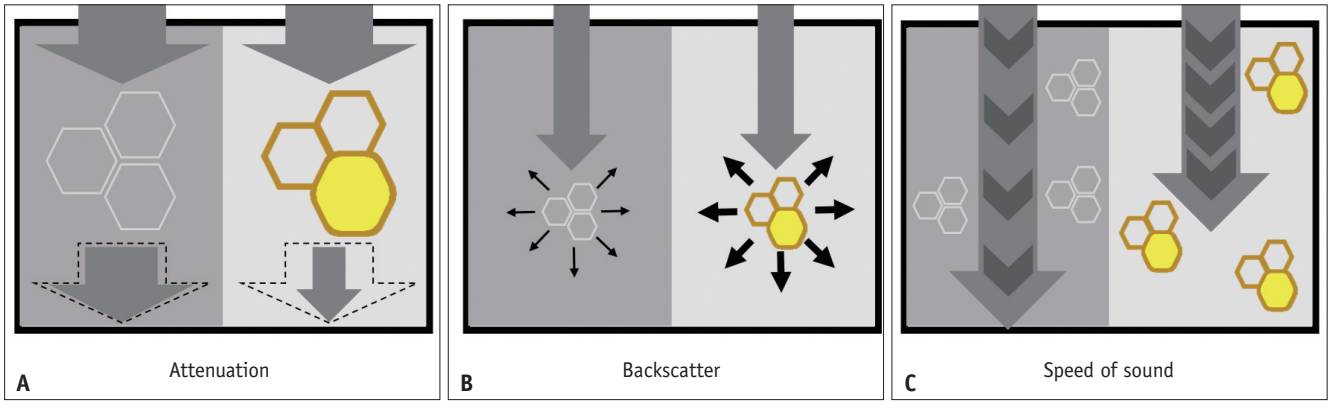

Fig. 3. Schematic figures illustrating the physical meanings of quantitative ultrasound parameters. Ultrasound wave, normal hepatocytes, and hepatocytes with fat accumulation are illustrated as arrows and hexagons with white and brown borders, respectively. **A.** Ultrasound waves lose energy when they pass through the liver. Ultrasound waves lose more energy as they pass through fatty liver tissue than normal liver, resulting in a higher attenuation coefficient. **B.** Scattering occurs when an ultrasound wave hits the tissue microstructure of the liver. More scattering occurs in fatty liver tissue than in normal liver tissue, resulting in a higher backscatter coefficient. **C.** The speed of an ultrasound wave is slower in fatty liver tissue than in normal liver tissue.

https://doi.org/10.3348/kjr.2021.0112

patient should lie in the dorsal decubitus position with the right arm in maximum abduction. Then, an operator should place the appropriate probe on the intercostal space at the level of the right hepatic lobe [68]. Originally, a 3.5-MHz probe (M probe) was used to measure CAP, but a probe with a lower central frequency (XL probe, with a central frequency of 2.5 MHz) can be used with similar diagnostic performance, which can be useful for obese patients [69,70]. The probe should be placed in a portion of the liver with a > 6-cm thickness and without large vessels, and the placement can be assisted by ultrasound time-motion images. After the probe is placed at the appropriate site, acquisition of CAP and liver stiffness can be initiated by pressing the probe button [68]. The final CAP result is expressed as dB/m, which is correlated with the grade of hepatic steatosis [19]. The overall failure rate of CAP measurement using the M probe was reported to be 7.7%, which was associated with body mass index (BMI): 1.0%

Table 2. Summary of Studies Assessing Hepatic Steatosis Using CAP

Study	N	Probe	Reference Standard	Target Degree of Steatosis	Optimal Cutoff (dB/m)	AUROC	Sen (%)	Spe (%)
Sasso et al. [19]	115	M	Biopsy	≥ S1 (10%)	238	0.91	91	81
				≥ S2	259	0.95	89	86
				≥ S3	292	0.89	100	78
de Lédinghen et al. [73]	112	M	Biopsy	≥ S1 (10%)	266	0.84	69	85
				≥ S2	311	0.86	57	94
				≥ S3	318	0.93	87	91
Myers et al. [74]	153	M	Biopsy	≥ 10%	283	0.81	76	79
				≥ S1 (5%)	289	0.79	68	88
				≥ S2	288	0.76	85	62
				≥ S3	283	0.70	94	47
Masaki et al. [75]	155	M	Biopsy	≥ S1 (5%)	233	0.88	87	77
Chan et al. [76]	161	M	Biopsy	≥ S1 (5%)	263	0.97	92	94
				≥ S2	263	0.86	97	68
				≥ S3	281	0.75	100	53
Chon et al. [77]	135	M	Biopsy	≥ S1 (5%)	250	0.89	73	95
				≥ S2	299	0.89	82	86
				≥ S3	327	0.80	78	84
Shen et al. [78]	152	M	Biopsy	≥ S1 (5%)	253	0.92	89	83
				≥ S2	285	0.92	93	83
				≥ S3	310	0.88	92	79
Karlas et al. [79]	65	M	Biopsy	≥ S1 (5%)	234	0.93	93	87
				≥ S2	269	0.94	97	81
				≥ S3	301	0.82	82	76
de Lédinghen et al. [80]	261	M	Biopsy	≥ S2	310	0.80	79	71
				≥ S3	311	0.66	87	47
Eddowes et al. [81]	380	M, XL	Biopsy	≥ S1 (5%)	302	0.87	80	83
				≥ S2	331	0.77	70	76
				≥ S3	337	0.70	72	63
Oeda et al. [82]	122	M	Biopsy	≥ S2	267	0.64	93	36
				≥ S3	286	0.69	90	43
		XL	Biopsy	≥ S2	273	0.68	96	32
				≥ S3	302	0.71	84	48
Caussy et al. [83]	100	M	MRI-PDFF	≥ 5%	294	0.84	75	78
				≥ 10%	311	0.89	79	85
		XL	MRI-PDFF	≥ 5%	307	0.86	74	75
				≥ 10%	322	0.93	83	87

AUROC = area under the receiver operating characteristic curve, CAP = controlled attenuation parameter, PDFF = proton density fat fraction, Sen = sensitivity, Spe = specificity

https://doi.org/10.3348/kjr.2021.0112

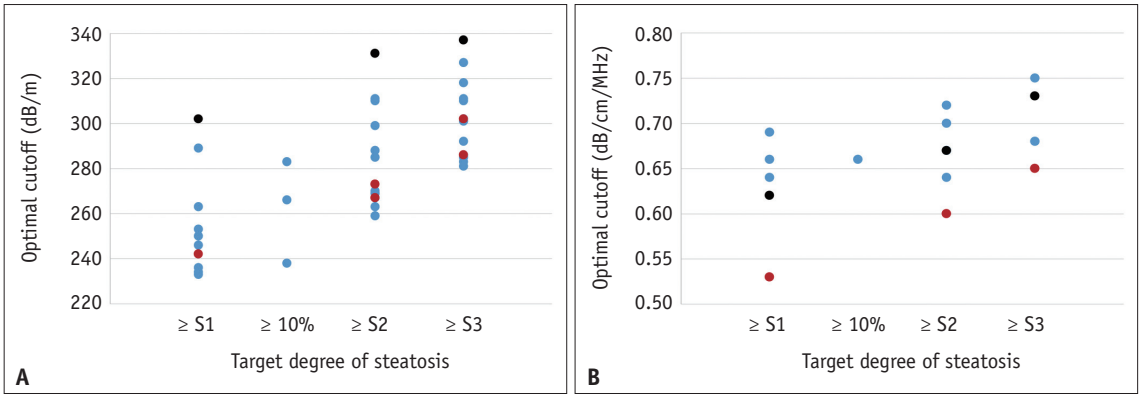

Fig. 4. Scatter plots for a cutoff value of (A) controlled attenuation parameter and (B) attenuation coefficient measured with B-mode ultrasound-guided attenuation imaging for different degrees of hepatic steatosis.
A. Blue, red, and black dots indicate cutoff values when using M probe, XL probe, and both M and XL probes, respectively. **B.** Blue, red, and black dots indicate cutoff values when using ATI (Canon Medical Systems), UGAP (GE Healthcare), ATT (Hitachi), respectively. Only studies using liver biopsy as a reference standard are included.

in patients with BMI ≤ 25 kg/m^2 and 58.4% in patients with BMI > 40 kg/m^2 [71]. The proper use of XL probes and automatic probe selection tools may reduce the failure rate [72].

The diagnostic performance of CAP has been variably reported as AUROCs ranging from 0.64 to > 0.90 (Table 2) [19,73-83]. In a meta-analysis of 19 studies involving 2735 patients, good overall diagnostic performance was reported as AUROCs of 0.823, 0.865, and 0.882 for the detection of hepatic steatosis grade ≥ S1, S2, and S3, respectively [84]. However, previous studies reported the inferiority of CAP to MRS (AUROC, 0.77 vs. 0.99 for ≥ S1) [34] or MRI-PDFF (AUROC, 0.88, 0.73, and 0.70 vs. 0.98, 0.90, and 0.79 for ≥ S1, S2, and S3, respectively) [85] for the diagnosis of hepatic steatosis.

Nevertheless, CAP is less time-consuming and allows the simultaneous evaluation of steatosis and fibrosis [86,87]. It is also likely to be observer-independent with good interobserver agreement (concordance correlation coefficient, 0.82 between two raters) [88]. However, CAP can be affected by several other factors, including skin capsular distance [82,89] and probe type (M vs. XL probe) [16,83] and the cutoff value for the diagnosis of hepatic steatosis is poorly standardized and variable across studies (Table 2, Fig. 4A). In addition, CAP measurement from a sample volume is obtained blindly without a B-mode ultrasound image; therefore, the CAP value can be misevaluated due to the inadvertent inclusion of hepatic vessels, ducts, masses, or uneven steatosis [87].

B-Mode Ultrasound-Guided Attenuation Imaging

The measurement of AC under B-mode ultrasound guidance has been studied since the 1980s [65,66,90]. Recently, novel techniques for calculating the AC under B-mode ultrasound guidance have been commercialized for the evaluation of hepatic steatosis, including attenuation imaging (ATI; Canon Medical Systems) [20], ultrasound-guided attenuation parameter (UGAP; GE Healthcare) [21], attenuation coefficient (ATT; Hitachi) [22], and tissue attenuation imaging (TAI; Samsung Medison) [23]. Although the detailed evaluation method slightly differs between vendors, the general process of measurement is as follows: 1) B-mode ultrasound evaluation of the liver is performed using a convex probe, 2) the probe is located to visualize the right hepatic lobe through an intercostal window for AC measurement, 3) the region of interest (ROI) is placed in the right hepatic lobe at least 2 cm below the liver capsule to avoid reverberation artifacts during breath-hold while avoiding or automatically excluding large vessels, and 4) AC value (in dB/cm/MHz) and reliability of the measurement (in R^2) are measured. A measurement of R^2 ≥ 0.60–0.90 is considered valid, depending on the vendors, and usually a median or mean value of five valid measurements is used for the assessment of hepatic steatosis (Fig. 5) [20-23,91]. The technical failure rate of these techniques, including ATI and UGAP, seems to be low (0%–4.3%), although there is little reported data [20,21,91-93].

In several recent studies, AC calculated with these techniques generally showed a good diagnostic performance for hepatic steatosis, with liver biopsy or MRI-PDFF as reference standards (AUROC, 0.76–0.98 with different

 https://doi.org/10.3348/kjr.2021.0112

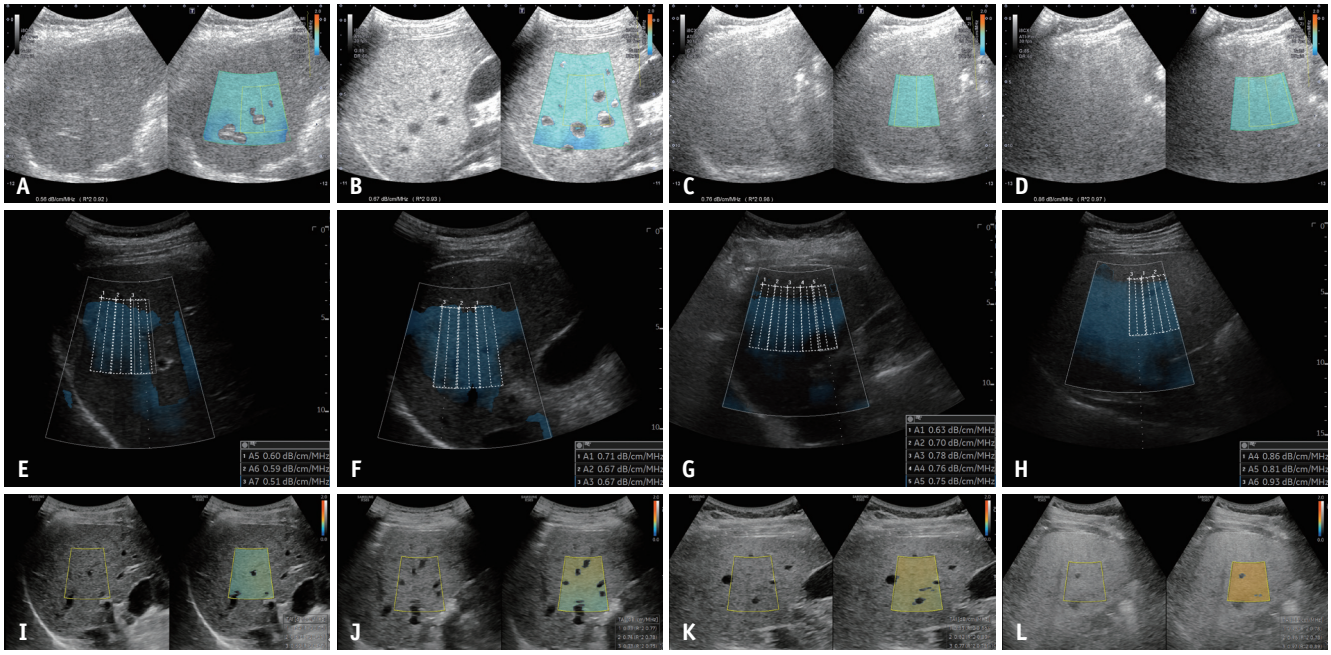

Fig. 5. Various commercialized techniques for B-mode ultrasound-guided attenuation imaging.
A-D. ATI (Canon Medical Systems) of patients **(A)** without hepatic steatosis, and with **(B)** mild, **(C)** moderate, and **(D)** severe hepatic steatosis, which were confirmed by liver biopsy. Median ACs are measured as **(A)** 0.56, **(B)** 0.67, **(C)** 0.76, and **(D)** 0.86 dB/cm/MHz, respectively. **E-H.** UGAP (GE Healthcare) of patients **(E)** without hepatic steatosis, and with **(F)** mild, **(G)** moderate, and **(H)** severe hepatic steatosis, which are estimated by controlled attenuation parameter. Median ACs are measured by **(E)** 0.59, **(F)** 0.67, **(G)** 0.77, and **(H)** 0.85 dB/cm/MHz, respectively. **I-L.** TAI (Samsung Medison) of patients **(I)** without hepatic steatosis and with **(J)** mild, **(K)** moderate, and **(L)** severe hepatic steatosis, which were confirmed by MRI-proton density fat fraction. Median ACs are measured by **(I)** 0.62, **(J)** 0.73, **(K)** 0.80, and **(L)** 0.97 dB/cm/MHz, respectively. AC = attenuation coefficient

techniques, reference standards, and target degree of steatosis) [20-22,91-98]. In addition, AC has been shown to correlate well with the degree of steatosis evaluated by histology or MRI-PDFF (r = 0.47–0.78) [20-22,91-97]. The detailed results of the studies on ATI, UGAP, ATT, and TAI are summarized in Table 3 and Figure 4B.

The advantage of these techniques over CAP is their use of B-mode ultrasound images. First, conventional ultrasound evaluation of the liver can be performed simultaneously with fat quantification. Second, the ROI for calculating AC can be placed while visualizing the liver, and a more reliable result can be obtained by avoiding large vessels, ducts, and hepatic masses or cysts [20-22]. Studies have shown that ATI and UGAP are superior to CAP for the prediction of hepatic steatosis [21,91]. In addition, ATI, UGAP, and TAI showed high intra- and inter-observer reproducibility (intraclass correlation coefficients [ICCs] for intra-and inter-observer reproducibility, 0.93 and 0.79 for ATI, 0.86 and 0.84 for UGAP, and 0.99 and 0.99 for TAI, respectively) [21,23,99]. However, AC can also theoretically be affected by fibrosis, although the effect of fibrosis is less pronounced than steatosis [20]. Different results have been reported on the effects of hepatic fibrosis on AC measured with ATI, UGAP, or TAI [92,93,97,100,101]. Therefore, further studies and standardization of AC, with consideration of concurrent hepatic fibrosis, are warranted.

Backscatter Coefficient (BSC)

BSC is a quantitative measure of ultrasound energy reflected from a tissue during ultrasound examination and is related to the echogenicity or "brightness" of the tissue in conventional ultrasound. As echogenicity increases with fatty liver in conventional ultrasound, BSC is also known to increase with hepatic fat infiltration [66,67]. In some recent studies, BSC correlated well with the degree of hepatic steatosis evaluated by liver biopsy (r = 0.67) [67] or MRI-PDFF (r = 0.72 and 0.80) [67,102]. BSC has also been reported to have a good diagnostic performance for hepatic steatosis (AUROC, 0.85 and 0.83 for ≥ S2 and ≥ S3 and 0.95 for MRI-PDFF ≥ 5%) [67,102], with biopsy or MRI-PDFF as reference standards. However, these studies were in the research stage, which required post-processing of QUS data using a custom software.

https://doi.org/10.3348/kjr.2021.0112

Korean Journal of Radiology
KJR

Table 3. Summary of Studies Assessing Hepatic Steatosis Using B-Mode Ultrasound-Guided Attenuation Imaging

Study	N	Technique	Reference Standard	*r*	Target Degree of Steatosis	Optimal Cutoff (dB/cm/MHz)	AUROC	Sen (%)	Spe (%)
Bae et al. [20]	108	ATI (Canon)	Biopsy	0.66	≥ S1 (5%)	0.64	0.84	75	77
					≥ 10%	0.66	0.88	80	83
					≥ S2	0.70	0.89	86	81
					≥ S3	0.75	0.93	100	82
Tada et al. [98]	148	ATI (Canon)	Biopsy	No data	≥ S1 (5%)	0.66	0.85	68	88
					≥ S2	0.67	0.91	92	84
					≥ S3	0.68	0.91	100	75
Jeon et al. [92]	87	ATI (Canon)	MRI-PDFF	0.66	≥ 5%	0.59	0.76	88	62
					≥ 10%	0.65	0.88	85	72
Dioguardi Burgio et al. [93]	101	ATI (Canon)	Biopsy	0.58	≥ S1 (5%)	0.69	0.81	76	86
					≥ S2	0.72	0.89	96	74
Jesper et al. [94]	27	ATI (Canon)	Biopsy	0.65	≥ S2	0.64	0.98	90	94
					≥ S3	0.68	0.98	100	90
Tada et al. [95]	119	ATI (Canon)	MRI-PDFF	0.70	≥ S1 (5.2%)	0.63	0.81	68	86
					≥ S2 (11.3%)	0.73	0.87	79	91
					≥ S3 (17.1%)	0.75	0.94	93	89
Ferraioli et al. [91]	72	ATI-Pen (Canon)	MRI-PDFF	0.78	≥ 5%	0.69	0.90	79	96
		ATI-Gen (Canon)	MRI-PDFF	0.83	≥ 5%	0.62	0.92	81	96
Fujiwara et al. [21]	163	UGAP (GE Healthcare)	Biopsy	0.78	≥ S1 (5%)	0.53	0.90	81	87
					≥ S2	0.60	0.95	86	82
					≥ S3	0.65	0.96	80	90
Tada et al. [96]	126	UGAP (GE Healthcare)	MRI-PDFF	0.75	≥ S1 (5.2%)	0.60	0.92	86	89
					≥ S2 (11.3%)	0.69	0.87	83	81
					≥ S3 (17.1%)	0.69	0.89	97	71
Tamaki et al. [22]	351	ATT (Hitachi)	Biopsy	0.47	≥ S1 (5%)	0.62	0.79	72	72
					≥ S2	0.67	0.87	82	82
					≥ S3	0.73	0.96	87	89
Jeon et al. [97]	120	TAI (Samsung)	MRI-PDFF	0.66	≥ 5%	0.88	0.86	78	79
					≥ 10%	0.98	0.84	64	93

AUROC = area under the receiver operating characteristic curve, PDFF = proton density fat fraction, *r* = correlation coefficient, Sen = sensitivity, Spe = specificity

Ultrasound Envelope Statistic Parametric Imaging (Speckle Statistics)

Ultrasound images contain speckle patterns that appear in a granular form. Since the speckle pattern is generated by the scattering of ultrasound signals by microstructures in the tissue, speckle statistics with the backscatter envelope can describe the scattering characteristics of the tissue [49,50,87]. The Rayleigh distribution generally describes the envelope of the backscattered ultrasound signal, which corresponds to the distribution of the envelope in the case of a high density of random scatterers without a coherent signal component [103,104]. However, because the distribution of the scattered ultrasound signals within the actual tissue does not always follow the Rayleigh distribution, various statistical models have been proposed [103-107]. Acoustic structure quantification (ASQ) and the Nakagami distribution have been the most widely studied for tissue characteristics.

Acoustic Structure Quantification (ASQ)

ASQ (Canon Medical Systems) is a quantification method for liver tissue characterization that measures the difference between the theoretical and real envelope distributions [108]. In ASQ, envelopes are used to compute C_m^2 by comparing the variance of the theoretical Rayleigh distribution and the real backscatter envelope distribution. Using limited envelope signals less than $\mu + 4\sigma$, where μ and σ denote the mean and standard deviation of the envelope distribution, respectively, C_m^2 is recalculated as rC_m^2. The recalculated rC_m^2 and the original C_m^2 are compared

 https://doi.org/10.3348/kjr.2021.0112

to derive the focal disturbance ratio (FD ratio) [24,50,109]. In fatty liver, the echogenicity of the hepatic parenchyma is increased, and the hepatic vessel walls are blurred due to reflection and scattering of the ultrasound waves, which results in the homogenization of the signal strength [24]. Therefore, the FD ratio theoretically decreases in fatty liver [24].

The process of performing ASQ examination is as follows. First, B-mode ultrasound evaluation of the liver is performed. Next, ultrasound images in ASQ mode are acquired from the right intercostal and right subcostal view 3–5 times each. Display depth and transmit focus are set to 10 cm and 6 cm, respectively. Then, ROIs that are as large as possible are placed on the liver in the images, while avoiding large hepatic vessels and artifacts. Finally, the FD ratio is calculated automatically within the ROI and displayed on the monitor. The mean FD ratio can be used for analysis of hepatic steatosis [108,110]. The FD ratio measured in the intercostal and subcostal views did not show a significant difference and showed good agreement (ICC, 0.90) [108].

In early animal and human studies, the FD ratio measured by ASQ correlated well with the fat droplet area on biopsy (r = -0.75 to -0.72) [24,111] or MRS (r = -0.90 to -0.87) [108,110,112]. One study also showed good diagnostic performance of the FD ratio (AUROC, 0.96 for hepatic steatosis ≥ 10%) [108]. However, another clinical study showed a relatively weak correlation between the FD ratio and MRS (r = -0.43) and fair diagnostic performance of the FD ratio for the diagnosis of hepatic steatosis, defined by a CAP value of > 300 dB/m (AUROC, 0.76) [113]. Furthermore, there have also been several studies on the relationship between FD ratio and fibrosis, although the results are controversial, which can be a confounding factor when evaluating hepatic steatosis using ASQ [112-116]. Further studies on both steatosis and fibrosis are needed.

Nakagami Imaging

The Nakagami distribution is a generalized statistical model for evaluating the scattering characteristics within a tissue [50,104]. The Nakagami parameter (m) of the distribution is a shape parameter that depends only on the shape of the envelope distribution. The Nakagami parameter encompasses most scattering conditions. For m < 1, the envelope statistics represent a small number of randomly distributed scatterers. When m = 1, the envelope statistic is a Rayleigh distribution and represents a large number of randomly distributed scatterers. When m > 1, the envelope statistics represent a large number of randomly distributed scatterers with additional periodic scatterers [50,104]. Therefore, the backscattering characteristics of liver steatosis can be explained by the Nakagami parameter with specific physical meanings according to the various amounts and spatial arrangement of scatterers.

Early animal and human studies revealed a significant positive correlation between the Nakagami parameter and the lipid concentration of the liver tissue (r = 0.86 and 0.79 for cholesterol and triglyceride, respectively) [117] and the degree of hepatic steatosis assessed by a conventional ultrasound-based scoring system (r = 0.84) [118].

Recently, a commercially available QUS modality based on the Nakagami distribution, tissue scatter-distribution imaging (TSI, Samsung Medison), was introduced (Fig. 6) [23,97,101]. The image acquisition process of TSI is similar to that of TAI. First, B-mode ultrasound images are acquired at the right hepatic lobe through the intercostal window near the level of the hepatic hilum. Then, a function key for the TSI is selected and an ROI box is generated. The operator should place the ROI in a relatively homogeneous region in the right hepatic lobe, at least 2 cm below the liver capsule. Large hepatic vessels, focal fat sparing or deposition, and artifacts should be avoided as for other QUS techniques, including TAI. Finally, the TSI parameter (TSI-p, which is equal to m x 100) is calculated and the mean or median values of TSI-p are used for the analysis of hepatic steatosis [23].

In recent studies, the TSI-p showed a good correlation with both CAP (r = 0.68, with CAP value [23], and r = 0.59 with steatosis grade determined by CAP [101]) and MRI-PDFF (r = 0.73) [97]. TSI also showed excellent performance for the diagnosis of hepatic steatosis (AUROC, 0.96 for hepatic fat content ≥ 5% and 0.94 for hepatic fat content ≥ 10%), with MRI-PDFF as a reference standard [97] and good intra- and inter-observer agreements (ICC, 0.98 and 0.95, respectively) [23]. However, there are controversial results on the effect of TSI-p on fibrosis, which is another important pathological feature of NAFLD/NASH [97,101]. Therefore, further validation with consideration of fibrosis is warranted.

Discussion and Future Development

For the diagnosis of hepatic steatosis, MRI-PDFF (sensitivity, 93%; specificity, 94% for ≥ S1) [45] and MRS

https://doi.org/10.3348/kjr.2021.0112

Korean Journal of Radiology
KJR

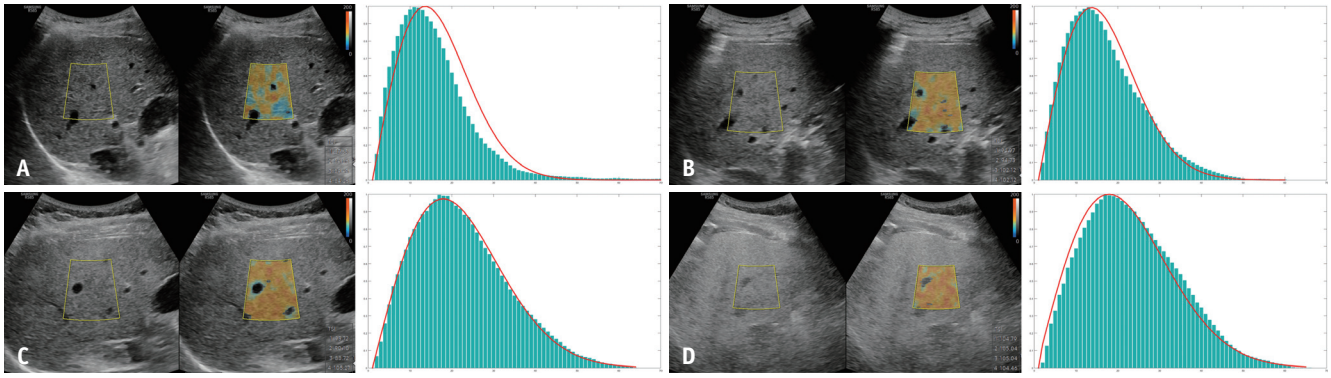

Fig. 6. A commercialized quantitative ultrasound technique based on Nakagami distribution–TSI (Samsung Medison).
A. TSI image (left) and corresponding histogram of the scattered ultrasound signals (right) in a patient without hepatic steatosis. Median TSI-p was calculated as 84.26. The histogram shows pre-Rayleigh distribution compared to the ideal Rayleigh distribution (red curve). **B.** TSI image (left) and corresponding histogram (right) in a patient with mild hepatic steatosis. Median TSI-p was calculated as 94.69. The histogram shows pre-Rayleigh distribution compared to the ideal Rayleigh distribution (red curve). **C.** TSI image (left) and corresponding histogram (right) in a patient with moderate hepatic steatosis. Median TSI-p was calculated as 100.44. The histogram is similar to the ideal Rayleigh distribution (red curve). **D.** TSI image (left) and corresponding histogram (right) in a patient with severe hepatic steatosis. Median TSI-p was calculated as 107.14. The histogram shows the post-Rayleigh distribution compared to the ideal Rayleigh distribution (red curve). Fat signal fractions measured with MRI-proton density fat fraction in these patients were **(A)** 3.1%, **(B)** 7.1%, **(C)** 12.6%, and **(D)** 25.2%, respectively.
TSI = tissue scatter-distribution imaging, TSI-p = TSI-parameter

(sensitivity, 88.5%; specificity, 92.0% for ≥ 0%–5%) [27] are the most accurate among imaging modalities, while CT is much less sensitive than MR-based methods (sensitivity, 46.1%; specificity, 93.5% for ≥ 0%–5%) [27]. Although variably reported in different studies, CAP and B-mode ultrasound-guided attenuation imaging seems to be more sensitive than CT, but less accurate than MR-based methods (Tables 2, 3). Meanwhile, ASQ and TSI showed excellent performance with MRS or MRI-PDFF as reference standards in each single prospective study (ASQ, sensitivity, 86.2% and specificity, 100% for ≥ 10% [108]; TSI, sensitivity, 85.7% and specificity, 97.4% for ≥ 5% [97]). However, larger multicenter studies are needed to validate these findings.

Although MRI-PDFF and MRS are the most accurate, reproducible, and well-validated methods for liver fat quantification, they are not routinely used for NAFLD screening because of their limited accessibility and low cost-effectiveness [38,119]. Considering the growing incidence of NAFLD, a more available, cost-effective, and easy-to-operate noninvasive diagnostic tool for the evaluation of hepatic steatosis is needed. Ultrasound is recommended as the first-line diagnostic method for assessing steatosis; however, it is limited by its relatively low sensitivity and substantial intra- and inter-observer variability [27,28]. Meanwhile, QUS generally showed good intra- and inter-observer agreements regardless of the technique used [21,23,88,99]. Furthermore, QUS provides continuous values related to hepatic fat content, unlike conventional ultrasound, which can provide only subjective categorical values; this can be useful for longitudinal follow-up and evaluation of treatment response [97]. In this context, QUS is a promising tool for screening and treatment monitoring of patients with NAFLD. In addition to NAFLD, QUS can potentially be applied to any condition where hepatic fat accumulation affects the prognosis of patients. For example, steatosis of ≥ 30% in a liver graft is associated with an increased risk of graft loss after liver transplantation [120]. In addition, the severity of hepatic steatosis is associated with patient outcomes and mortality after liver surgery [121]. Therefore, QUS techniques can potentially be used as a non-invasive preoperative or pre-transplantation evaluation tool for the presence and degree of hepatic steatosis. Various QUS techniques, including CAP [19], attenuation imaging [20-23], ASQ [24], and Nakagami imaging [23], have been commercialized, and have shown promising results for quantitative evaluation of hepatic steatosis, although further validation and standardization between vendors or platforms are needed for clinical adoption.

Inflammation and fibrosis are also important histologic features of NAFLD, which can affect the treatment strategy [122]. Although transient elastography is a well-validated method for the evaluation of hepatic fibrosis [123-125], it is limited by blinded evaluation without B-mode ultrasound guidance. ASQ has been studied for the evaluation of fibrosis; however, its performance, as

 https://doi.org/10.3348/kjr.2021.0112

mentioned earlier, is controversial [113-116]. Thus, there is a need for noninvasive evaluation of inflammation or fibrosis in patients with NASH/NAFLD. Recently, shear-wave elastography and shear-wave dispersion imaging (viscosity imaging) based on ultrasound have shown good outcomes for detection of fibrosis [126,127] and inflammation [128,129], respectively. These techniques, in conjunction with QUS techniques for hepatic fat quantification, may enable comprehensive evaluation of patients with NASH/NAFLD using ultrasound. Further studies validating these imaging-based biomarkers in a large independent group are needed.

Availability of Data and Material

Data sharing does not apply to this article as no datasets were generated or analyzed during the current study.

Conflicts of Interest

Jeong Min Lee received grants from Bayer Healthcare, Canon Healthcare, Philips Healthcare, GE Healthcare, CMS, Guerbet, Samsung Medison, Bracco, personal fees from Bayer Healthcare, Siemens Healthineer, Samsung Medison, Guerbet, outside the submitted work. Gunwoo Lee is employee of Samsung Electronics Co., Ltd. Other authors have no conflict of interest to disclose.
Jeong Min Lee who is on the editorial board of the *Korean Journal of Radiology* was not involved in the editorial evaluation or decision to publish this article.

Author Contributions

Conceptualization: Jeong Min Lee. Data curation: Junghoan Park, Gunwoo Lee, Sun Kyung Jeon, Ijin Joo. Funding acquisition: Jeong Min Lee. Investigation: all authors. Project administration: Jeong Min Lee. Supervision: Jeong Min Lee. Writing—original draft: Junghoan Park. Writing—review & editing: Jeong Min Lee, Gunwoo Lee, Sun Kyung Jeon, Ijin Joo.

ORCID iDs

Junghoan Park
https://orcid.org/0000-0002-0636-3756
Jeong Min Lee
https://orcid.org/0000-0003-0561-8777
Gunwoo Lee
https://orcid.org/0000-0002-7826-0035
Sun Kyung Jeon
https://orcid.org/0000-0002-8991-3986
Ijin Joo
https://orcid.org/0000-0002-1341-4072

Funding Statement

This work was supported by Samsung Medison (Project No. 06-2020-2040).

REFERENCES

1. Angulo P. Nonalcoholic fatty liver disease. *N Engl J Med* 2002;346:1221-1231
2. Serfaty L, Lemoine M. Definition and natural history of metabolic steatosis: clinical aspects of NAFLD, NASH and cirrhosis. *Diabetes Metab* 2008;34:634-637
3. Hashimoto E, Taniai M, Tokushige K. Characteristics and diagnosis of NAFLD/NASH. *J Gastroenterol Hepatol* 2013;28 Suppl 4:64-70
4. Bellentani S. The epidemiology of non-alcoholic fatty liver disease. *Liver Int* 2017;37 Suppl 1:81-84
5. Younossi ZM, Stepanova M, Younossi Y, Golabi P, Mishra A, Rafiq N, et al. Epidemiology of chronic liver diseases in the USA in the past three decades. *Gut* 2020;69:564-568
6. Younossi ZM, Stepanova M, Afendy M, Fang Y, Younossi Y, Mir H, et al. Changes in the prevalence of the most common causes of chronic liver diseases in the United States from 1988 to 2008. *Clin Gastroenterol Hepatol* 2011;9:524-530.e1
7. Fan JG, Kim SU, Wong VW. New trends on obesity and NAFLD in Asia. *J Hepatol* 2017;67:862-873
8. Chang Y, Jung HS, Yun KE, Cho J, Cho YK, Ryu S. Cohort study of non-alcoholic fatty liver disease, NAFLD fibrosis score, and the risk of incident diabetes in a Korean population. *Am J Gastroenterol* 2013;108:1861-1868
9. McPherson S, Hardy T, Henderson E, Burt AD, Day CP, Anstee QM. Evidence of NAFLD progression from steatosis to fibrosing-steatohepatitis using paired biopsies: implications for prognosis and clinical management. *J Hepatol* 2015;62:1148-1155
10. Arulanandan A, Ang B, Bettencourt R, Hooker J, Behling C, Lin GY, et al. Association between quantity of liver fat and cardiovascular risk in patients with nonalcoholic fatty liver disease independent of nonalcoholic steatohepatitis. *Clin Gastroenterol Hepatol* 2015;13:1513-1520.e1
11. Hossain N, Kanwar P, Mohanty SR. A comprehensive updated review of pharmaceutical and nonpharmaceutical treatment for NAFLD. *Gastroenterol Res Pract* 2016;2016:7109270
12. Gordon A, McLean CA, Pedersen JS, Bailey MJ, Roberts SK. Hepatic steatosis in chronic hepatitis B and C: predictors, distribution and effect on fibrosis. *J Hepatol* 2005;43:38-44
13. Rinella ME, Sanyal AJ. Management of NAFLD: a stage-based approach. *Nat Rev Gastroenterol Hepatol* 2016;13:196-205
14. Wong VW, Adams LA, de Lédinghen V, Wong GL, Sookoian S. Noninvasive biomarkers in NAFLD and NASH - current progress and future promise. *Nat Rev Gastroenterol Hepatol*

2018;15:461-478
15. Kramer H, Pickhardt PJ, Kliewer MA, Hernando D, Chen GH, Zagzebski JA, et al. Accuracy of liver fat quantification with advanced CT, MRI, and ultrasound techniques: prospective comparison with MR spectroscopy. *AJR Am J Roentgenol* 2017;208:92-100
16. Caussy C, Alquiraish MH, Nguyen P, Hernandez C, Cepin S, Fortney LE, et al. Optimal threshold of controlled attenuation parameter with MRI-PDFF as the gold standard for the detection of hepatic steatosis. *Hepatology* 2018;67:1348-1359
17. Ferraioli G, Maiocchi L, Raciti MV, Tinelli C, De Silvestri A, Nichetti M, et al. Detection of liver steatosis with a novel ultrasound-based technique: a pilot study using MRI-derived proton density fat fraction as the gold standard. *Clin Transl Gastroenterol* 2019;10:e00081
18. Hernaez R, Lazo M, Bonekamp S, Kamel I, Brancati FL, Guallar E, et al. Diagnostic accuracy and reliability of ultrasonography for the detection of fatty liver: a meta-analysis. *Hepatology* 2011;54:1082-1090
19. Sasso M, Beaugrand M, de Ledinghen V, Douvin C, Marcellin P, Poupon R, et al. Controlled attenuation parameter (CAP): a novel VCTE™ guided ultrasonic attenuation measurement for the evaluation of hepatic steatosis: preliminary study and validation in a cohort of patients with chronic liver disease from various causes. *Ultrasound Med Biol* 2010;36:1825-1835
20. Bae JS, Lee DH, Lee JY, Kim H, Yu SJ, Lee JH, et al. Assessment of hepatic steatosis by using attenuation imaging: a quantitative, easy-to-perform ultrasound technique. *Eur Radiol* 2019;29:6499-6507
21. Fujiwara Y, Kuroda H, Abe T, Ishida K, Oguri T, Noguchi S, et al. The B-mode image-guided ultrasound attenuation parameter accurately detects hepatic steatosis in chronic liver disease. *Ultrasound Med Biol* 2018;44:2223-2232
22. Tamaki N, Koizumi Y, Hirooka M, Yada N, Takada H, Nakashima O, et al. Novel quantitative assessment system of liver steatosis using a newly developed attenuation measurement method. *Hepatol Res* 2018;48:821-828
23. Jeon SK, Lee JM, Joo I. Clinical feasibility of quantitative ultrasound imaging for suspected hepatic steatosis: intra- and inter-examiner reliability and correlation with controlled attenuation parameter. *Ultrasound Med Biol* 2021;47:438-445
24. Kuroda H, Kakisaka K, Kamiyama N, Oikawa T, Onodera M, Sawara K, et al. Non-invasive determination of hepatic steatosis by acoustic structure quantification from ultrasound echo amplitude. *World J Gastroenterol* 2012;18:3889-3895
25. Ghoshal G, Lavarello RJ, Kemmerer JP, Miller RJ, Oelze ML. Ex vivo study of quantitative ultrasound parameters in fatty rabbit livers. *Ultrasound Med Biol* 2012;38:2238-2248
26. Saadeh S, Younossi ZM, Remer EM, Gramlich T, Ong JP, Hurley M, et al. The utility of radiological imaging in nonalcoholic fatty liver disease. *Gastroenterology* 2002;123:745-750
27. Bohte AE, van Werven JR, Bipat S, Stoker J. The diagnostic accuracy of US, CT, MRI and 1H-MRS for the evaluation of hepatic steatosis compared with liver biopsy: a meta-analysis. *Eur Radiol* 2011;21:87-97
28. Strauss S, Gavish E, Gottlieb P, Katsnelson L. Interobserver and intraobserver variability in the sonographic assessment of fatty liver. *AJR Am J Roentgenol* 2007;189:W320-W323
29. Yajima Y, Narui T, Ishii M, Abe R, Ohtsuki M, Goto Y, et al. Computed tomography in the diagnosis of fatty liver: total lipid content and computed tomography number. *Tohoku J Exp Med* 1982;136:337-342
30. Hamer OW, Aguirre DA, Casola G, Lavine JE, Woenckhaus M, Sirlin CB. Fatty liver: imaging patterns and pitfalls. *Radiographics* 2006;26:1637-1653
31. Kodama Y, Ng CS, Wu TT, Ayers GD, Curley SA, Abdalla EK, et al. Comparison of CT methods for determining the fat content of the liver. *AJR Am J Roentgenol* 2007;188:1307-1312
32. Limanond P, Raman SS, Lassman C, Sayre J, Ghobrial RM, Busuttil RW, et al. Macrovesicular hepatic steatosis in living related liver donors: correlation between CT and histologic findings. *Radiology* 2004;230:276-280
33. Ma X, Holalkere NS, Kambadakone R A, Mino-Kenudson M, Hahn PF, Sahani DV. Imaging-based quantification of hepatic fat: methods and clinical applications. *Radiographics* 2009;29:1253-1277
34. Runge JH, Smits LP, Verheij J, Depla A, Kuiken SD, Baak BC, et al. MR spectroscopy–derived proton density fat fraction is superior to controlled attenuation parameter for detecting and grading hepatic steatosis. *Radiology* 2018;286:547-556
35. van Werven JR, Marsman HA, Nederveen AJ, Smits NJ, ten Kate FJ, van Gulik TM, et al. Assessment of hepatic steatosis in patients undergoing liver resection: comparison of US, CT, T1-weighted dual-echo MR imaging, and point-resolved 1H MR spectroscopy. *Radiology* 2010;256:159-168
36. Cassidy FH, Yokoo T, Aganovic L, Hanna RF, Bydder M, Middleton MS, et al. Fatty liver disease: MR imaging techniques for the detection and quantification of liver steatosis. *Radiographics* 2009;29:231-260
37. Qayyum A. MR spectroscopy of the liver: principles and clinical applications. *Radiographics* 2009;29:1653-1664
38. Reeder SB, Cruite I, Hamilton G, Sirlin CB. Quantitative assessment of liver fat with magnetic resonance imaging and spectroscopy. *J Magn Reson Imaging* 2011;34:729-749
39. Caussy C, Reeder SB, Sirlin CB, Loomba R. Noninvasive, quantitative assessment of liver fat by MRI-PDFF as an endpoint in NASH trials. *Hepatology* 2018;68:763-772
40. Hood MN, Ho VB, Smirniotopoulos JG, Szumowski J. Chemical shift: the artifact and clinical tool revisited. *Radiographics* 1999;19:357-371
41. Dixon WT. Simple proton spectroscopic imaging. *Radiology* 1984;153:189-194
42. Ma J. Dixon techniques for water and fat imaging. *J Magn*

https://doi.org/10.3348/kjr.2021.0112

Reson Imaging 2008;28:543-558
43. Liu CY, McKenzie CA, Yu H, Brittain JH, Reeder SB. Fat quantification with IDEAL gradient echo imaging: correction of bias from T(1) and noise. *Magn Reson Med* 2007;58:354-364
44. Yu H, Shimakawa A, McKenzie CA, Brodsky E, Brittain JH, Reeder SB. Multiecho water-fat separation and simultaneous R2* estimation with multifrequency fat spectrum modeling. *Magn Reson Med* 2008;60:1122-1134
45. Gu J, Liu S, Du S, Zhang Q, Xiao J, Dong Q, et al. Diagnostic value of MRI-PDFF for hepatic steatosis in patients with non-alcoholic fatty liver disease: a meta-analysis. *Eur Radiol* 2019;29:3564-3573
46. Idilman IS, Keskin O, Celik A, Savas B, Elhan AH, Idilman R, et al. A comparison of liver fat content as determined by magnetic resonance imaging-proton density fat fraction and MRS versus liver histology in non-alcoholic fatty liver disease. *Acta Radiol* 2016;57:271-278
47. Mamou J, Oelze ML. *Quantitative ultrasound in soft tissues*, 1st ed. Dordrecht: Springer, 2013:xi-xiii
48. Labyed Y, Bigelow TA. A theoretical comparison of attenuation measurement techniques from backscattered ultrasound echoes. *J Acoust Soc Am* 2011;129:2316-2324
49. Oelze ML, Mamou J. Review of quantitative ultrasound: envelope statistics and backscatter coefficient imaging and contributions to diagnostic ultrasound. *IEEE Trans Ultrason Ferroelectr Freq Control* 2016;63:336-351
50. Zhou Z, Zhang Q, Wu W, Wu S, Tsui PH. Hepatic steatosis assessment using quantitative ultrasound parametric imaging based on backscatter envelope statistics. *Appl Sci* 2019;9:661
51. Jakovljevic M, Hsieh S, Ali R, Chau Loo Kung G, Hyun D, Dahl JJ. Local speed of sound estimation in tissue using pulse-echo ultrasound: model-based approach. *J Acoust Soc Am* 2018;144:254-266
52. Byram BC, Trahey GE, Jensen JA. A method for direct localized sound speed estimates using registered virtual detectors. *Ultrason Imaging* 2012;34:159-180
53. Sigrist RMS, Liau J, Kaffas AE, Chammas MC, Willmann JK. Ultrasound elastography: review of techniques and clinical applications. *Theranostics* 2017;7:1303-1329
54. Barry CT, Mills B, Hah Z, Mooney RA, Ryan CK, Rubens DJ, et al. Shear wave dispersion measures liver steatosis. *Ultrasound Med Biol* 2012;38:175-182
55. Glüer CC. Quantitative ultrasound techniques for the assessment of osteoporosis: expert agreement on current status. *J Bone Miner Res* 1997;12:1280-1288
56. Di Bello V, Talarico L, Picano E, Di Muro C, Landini L, Paterni M, et al. Increased echodensity of myocardial wall in the diabetic heart: an ultrasound tissue characterization study. *J Am Coll Cardiol* 1995;25:1408-1415
57. Sadigh G, Carlos RC, Neal CH, Dwamena BA. Accuracy of quantitative ultrasound elastography for differentiation of malignant and benign breast abnormalities: a meta-analysis. *Breast Cancer Res Treat* 2012;134:923-931
58. Tadayyon H, Sadeghi-Naini A, Wirtzfeld L, Wright FC, Czarnota G. Quantitative ultrasound characterization of locally advanced breast cancer by estimation of its scatterer properties. *Med Phys* 2014;41:012903
59. Lavarello RJ, Ridgway WR, Sarwate SS, Oelze ML. Characterization of thyroid cancer in mouse models using high-frequency quantitative ultrasound techniques. *Ultrasound Med Biol* 2013;39:2333-2341
60. Rohrbach D, Wodlinger B, Wen J, Mamou J, Feleppa E. High-frequency quantitative ultrasound for imaging prostate cancer using a novel micro-ultrasound scanner. *Ultrasound Med Biol* 2018;44:1341-1354
61. Saegusa-Beecroft E, Machi J, Mamou J, Hata M, Coron A, Yanagihara ET, et al. Three-dimensional quantitative ultrasound for detecting lymph node metastases. *J Surg Res* 2013;183:258-269
62. Sadeghi-Naini A, Papanicolau N, Falou O, Zubovits J, Dent R, Verma S, et al. Quantitative ultrasound evaluation of tumor cell death response in locally advanced breast cancer patients receiving chemotherapy. *Clin Cancer Res* 2013;19:2163-2174
63. Tadayyon H, Sannachi L, Gangeh M, Sadeghi-Naini A, Tran W, Trudeau ME, et al. Quantitative ultrasound assessment of breast tumor response to chemotherapy using a multi-parameter approach. *Oncotarget* 2016;7:45094-45111
64. Ozturk A, Grajo JR, Gee MS, Benjamin A, Zubajlo RE, Thomenius KE, et al. Quantitative hepatic fat quantification in non-alcoholic fatty liver disease using ultrasound-based techniques: a review of literature and their diagnostic performance. *Ultrasound Med Biol* 2018;44:2461-2475
65. Taylor KJ, Riely CA, Hammers L, Flax S, Weltin G, Garcia-Tsao G, et al. Quantitative US attenuation in normal liver and in patients with diffuse liver disease: importance of fat. *Radiology* 1986;160:65-71
66. Lu ZF, Zagzebski JA, Lee FT. Ultrasound backscatter and attenuation in human liver with diffuse disease. *Ultrasound Med Biol* 1999;25:1047-1054
67. Paige JS, Bernstein GS, Heba E, Costa EAC, Fereirra M, Wolfson T, et al. A pilot comparative study of quantitative ultrasound, conventional ultrasound, and MRI for predicting histology-determined steatosis grade in adult nonalcoholic fatty liver disease. *AJR Am J Roentgenol* 2017;208:W168-W177
68. de Lédinghen V, Vergniol J. Transient elastography (FibroScan). *Gastroenterol Clin Biol* 2008;32:58-67
69. Sasso M, Audière S, Kemgang A, Gaouar F, Corpechot C, Chazouillères O, et al. Liver steatosis assessed by controlled attenuation parameter (CAP) measured with the XL probe of the FibroScan: a pilot study assessing diagnostic accuracy. *Ultrasound Med Biol* 2016;42:92-103
70. de Lédinghen V, Hiriart JB, Vergniol J, Merrouche W, Bedossa P, Paradis V. Controlled attenuation parameter (CAP) with the XL probe of the Fibroscan®: a comparative study with

https://doi.org/10.3348/kjr.2021.0112

the M probe and liver biopsy. *Dig Dis Sci* 2017;62:2569-2577
71. de Lédinghen V, Vergniol J, Capdepont M, Chermak F, Hiriart JB, Cassinotto C, et al. Controlled attenuation parameter (CAP) for the diagnosis of steatosis: a prospective study of 5323 examinations. *J Hepatol* 2014;60:1026-1031
72. Vuppalanchi R, Siddiqui MS, Van Natta ML, Hallinan E, Brandman D, Kowdley K, et al. Performance characteristics of vibration-controlled transient elastography for evaluation of nonalcoholic fatty liver disease. *Hepatology* 2018;67:134-144
73. de Lédinghen V, Vergniol J, Foucher J, Merrouche W, le Bail B. Non-invasive diagnosis of liver steatosis using controlled attenuation parameter (CAP) and transient elastography. *Liver Int* 2012;32:911-918
74. Myers RP, Pollett A, Kirsch R, Pomier-Layrargues G, Beaton M, Levstik M, et al. Controlled attenuation parameter (CAP): a noninvasive method for the detection of hepatic steatosis based on transient elastography. *Liver Int* 2012;32:902-910
75. Masaki K, Takaki S, Hyogo H, Kobayashi T, Fukuhara T, Naeshiro N, et al. Utility of controlled attenuation parameter measurement for assessing liver steatosis in Japanese patients with chronic liver diseases. *Hepatol Res* 2013;43:1182-1189
76. Chan WK, Nik Mustapha NR, Mahadeva S. Controlled attenuation parameter for the detection and quantification of hepatic steatosis in nonalcoholic fatty liver disease. *J Gastroenterol Hepatol* 2014;29:1470-1476
77. Chon YE, Jung KS, Kim SU, Park JY, Park YN, Kim DY, et al. Controlled attenuation parameter (CAP) for detection of hepatic steatosis in patients with chronic liver diseases: a prospective study of a native Korean population. *Liver Int* 2014;34:102-109
78. Shen F, Zheng RD, Mi YQ, Wang XY, Pan Q, Chen GY, et al. Controlled attenuation parameter for non-invasive assessment of hepatic steatosis in Chinese patients. *World J Gastroenterol* 2014;20:4702-4711
79. Karlas T, Petroff D, Garnov N, Böhm S, Tenckhoff H, Wittekind C, et al. Non-invasive assessment of hepatic steatosis in patients with NAFLD using controlled attenuation parameter and 1H-MR spectroscopy. *PLoS One* 2014;9:e91987
80. de Lédinghen V, Wong GL, Vergniol J, Chan HL, Hiriart JB, Chan AW, et al. Controlled attenuation parameter for the diagnosis of steatosis in non-alcoholic fatty liver disease. *J Gastroenterol Hepatol* 2016;31:848-855
81. Eddowes PJ, Sasso M, Allison M, Tsochatzis E, Anstee QM, Sheridan D, et al. Accuracy of FibroScan controlled attenuation parameter and liver stiffness measurement in assessing steatosis and fibrosis in patients with nonalcoholic fatty liver disease. *Gastroenterology* 2019;156:1717-1730
82. Oeda S, Takahashi H, Imajo K, Seko Y, Ogawa Y, Moriguchi M, et al. Accuracy of liver stiffness measurement and controlled attenuation parameter using FibroScan® M/XL probes to diagnose liver fibrosis and steatosis in patients with nonalcoholic fatty liver disease: a multicenter prospective study. *J Gastroenterol* 2020;55:428-440
83. Caussy C, Brissot J, Singh S, Bassirian S, Hernandez C, Bettencourt R, et al. Prospective, same-day, direct comparison of controlled attenuation parameter with the M vs the XL probe in patients with nonalcoholic fatty liver disease, using magnetic resonance imaging-proton density fat fraction as the standard. *Clin Gastroenterol Hepatol* 2020;18:1842-1850.e6
84. Karlas T, Petroff D, Sasso M, Fan JG, Mi YQ, de Lédinghen V, et al. Individual patient data meta-analysis of controlled attenuation parameter (CAP) technology for assessing steatosis. *J Hepatol* 2017;66:1022-1030
85. Imajo K, Kessoku T, Honda Y, Tomeno W, Ogawa Y, Mawatari H, et al. Magnetic resonance imaging more accurately classifies steatosis and fibrosis in patients with nonalcoholic fatty liver disease than transient elastography. *Gastroenterology* 2016;150:626-637.e7
86. Mikolasevic I, Orlic L, Franjic N, Hauser G, Stimac D, Milic S. Transient elastography (FibroScan®) with controlled attenuation parameter in the assessment of liver steatosis and fibrosis in patients with nonalcoholic fatty liver disease - where do we stand? *World J Gastroenterol* 2016;22:7236-7251
87. Pirmoazen AM, Khurana A, El Kaffas A, Kamaya A. Quantitative ultrasound approaches for diagnosis and monitoring hepatic steatosis in nonalcoholic fatty liver disease. *Theranostics* 2020;10:4277-4289
88. Ferraioli G, Tinelli C, Lissandrin R, Zicchetti M, Rondanelli M, Perani G, et al. Interobserver reproducibility of the controlled attenuation parameter (CAP) for quantifying liver steatosis. *Hepatol Int* 2014;8:576-581
89. Shen F, Zheng RD, Shi JP, Mi YQ, Chen GF, Hu X, et al. Impact of skin capsular distance on the performance of controlled attenuation parameter in patients with chronic liver disease. *Liver Int* 2015;35:2392-2400
90. Fujii Y, Taniguchi N, Itoh K, Shigeta K, Wang Y, Tsao JW, et al. A new method for attenuation coefficient measurement in the liver: comparison with the spectral shift central frequency method. *J Ultrasound Med* 2002;21:783-788
91. Ferraioli G, Maiocchi L, Savietto G, Tinelli C, Nichetti M, Rondanelli M, et al. Performance of the attenuation imaging technology in the detection of liver steatosis. *J Ultrasound Med* 2021;40:1325-1332
92. Jeon SK, Lee JM, Joo I, Yoon JH, Lee DH, Lee JY, et al. Prospective evaluation of hepatic steatosis using ultrasound attenuation imaging in patients with chronic liver disease with magnetic resonance imaging proton density fat fraction as the reference standard. *Ultrasound Med Biol* 2019;45:1407-1416
93. Dioguardi Burgio M, Ronot M, Reizine E, Rautou PE, Castera L, Paradis V, et al. Quantification of hepatic steatosis with ultrasound: promising role of attenuation imaging coefficient in a biopsy-proven cohort. *Eur Radiol* 2020;30:2293-2301
94. Jesper D, Klett D, Schellhaas B, Pfeifer L, Leppkes M,

 https://doi.org/10.3348/kjr.2021.0112

Waldner M, et al. Ultrasound-based attenuation imaging for the non-invasive quantification of liver fat-a pilot study on feasibility and inter-observer variability. *IEEE J Transl Eng Health Med* 2020;8:1800409
95. Tada T, Kumada T, Toyoda H, Nakamura S, Shibata Y, Yasuda S, et al. Attenuation imaging based on ultrasound technology for assessment of hepatic steatosis: a comparison with magnetic resonance imaging-determined proton density fat fraction. *Hepatol Res* 2020;50:1319-1327
96. Tada T, Kumada T, Toyoda H, Kobayashi N, Sone Y, Oguri T, et al. Utility of attenuation coefficient measurement using an ultrasound-guided attenuation parameter for evaluation of hepatic steatosis: comparison with MRI-determined proton density fat fraction. *AJR Am J Roentgenol* 2019;212:332-341
97. Jeon SK, Lee JM, Joo I, Park SJ. Quantitative ultrasound radiofrequency data analysis for the assessment of hepatic steatosis in nonalcoholic fatty liver disease using magnetic resonance imaging proton density fat fraction as the reference standard. *Korean J Radiol* 2021;22:1077-1086
98. Tada T, Iijima H, Kobayashi N, Yoshida M, Nishimura T, Kumada T, et al. Usefulness of attenuation imaging with an ultrasound scanner for the evaluation of hepatic steatosis. *Ultrasound Med Biol* 2019;45:2679-2687
99. Yoo J, Lee JM, Joo I, Lee DH, Yoon JH, Kang HJ, et al. Reproducibility of ultrasound attenuation imaging for the noninvasive evaluation of hepatic steatosis. *Ultrasonography* 2020;39:121-129
100. Tada T, Kumada T, Toyoda H, Yasuda S, Sone Y, Hashinokuchi S, et al. Liver stiffness does not affect ultrasound-guided attenuation coefficient measurement in the evaluation of hepatic steatosis. *Hepatol Res* 2020;50:190-198
101. Jeon SK, Joo I, Kim SY, Jang JK, Park J, Park HS, et al. Quantitative ultrasound radiofrequency data analysis for the assessment of hepatic steatosis using the controlled attenuation parameter as a reference standard. *Ultrasonography* 2021;40:136-146
102. Lin SC, Heba E, Wolfson T, Ang B, Gamst A, Han A, et al. Noninvasive diagnosis of nonalcoholic fatty liver disease and quantification of liver fat using a new quantitative ultrasound technique. *Clin Gastroenterol Hepatol* 2015;13:1337-1345.e6
103. Destrempes F, Cloutier G. A critical review and uniformized representation of statistical distributions modeling the ultrasound echo envelope. *Ultrasound Med Biol* 2010;36:1037-1051
104. Mohana Shankar P. A general statistical model for ultrasonic backscattering from tissues. *IEEE Trans Ultrason Ferroelectr Freq Control* 2000;47:727-736
105. Destrempes F, Porée J, Cloutier G. Estimation method of the homodyned K-distribution based on the mean intensity and two log-moments. *SIAM J Imaging Sci* 2013;6:1499-1530
106. Tsai YW, Zhou Z, Gong CA, Tai DI, Cristea A, Lin YC, et al. Ultrasound detection of liver fibrosis in individuals with hepatic steatosis using the homodyned K distribution. *Ultrasound Med Biol* 2021;47:84-94
107. Ma HY, Zhou Z, Wu S, Wan YL, Tsui PH. A computer-aided diagnosis scheme for detection of fatty liver in vivo based on ultrasound kurtosis imaging. *J Med Syst* 2016;40:33
108. Son JY, Lee JY, Yi NJ, Lee KW, Suh KS, Kim KG, et al. Hepatic steatosis: assessment with acoustic structure quantification of US imaging. *Radiology* 2016;278:257-264
109. Toyoda H, Kumada T, Kamiyama N, Shiraki K, Takase K, Yamaguchi T, et al. B-mode ultrasound with algorithm based on statistical analysis of signals: evaluation of liver fibrosis in patients with chronic hepatitis C. *AJR Am J Roentgenol* 2009;193:1037-1043
110. Lee DH, Lee JY, Park MS, Han JK. Non-invasive monitoring of hepatic steatosis via acoustic structure quantification of ultrasonography with MR spectroscopy as the reference standard. *Ultrasonography* 2020;39:70-78
111. Onodera M. The new non-invasive quantification of hepatic steatosis with morbid obesity by acoustic structure quantification (ASQ) from ultrasound echo amplitude. *Ultrasound Med Biol* 2013;39:S2
112. Lee DH, Lee JY, Lee KB, Han JK. Evaluation of hepatic steatosis by using acoustic structure quantification US in a rat model: comparison with pathologic examination and MR spectroscopy. *Radiology* 2017;285:445-453
113. Karlas T, Berger J, Garnov N, Lindner F, Busse H, Linder N, et al. Estimating steatosis and fibrosis: comparison of acoustic structure quantification with established techniques. *World J Gastroenterol* 2015;21:4894-4902
114. Ricci P, Marigliano C, Cantisani V, Porfiri A, Marcantonio A, Lodise P, et al. Ultrasound evaluation of liver fibrosis: preliminary experience with acoustic structure quantification (ASQ) software. *Radiol Med* 2013;118:995-1010
115. Huang Y, Wang Z, Liao B, Liang JY, Zhou LY, Wang F, et al. Assessment of liver fibrosis in chronic hepatitis B using acoustic structure quantification: quantitative morphological ultrasound. *Eur Radiol* 2016;26:2344-2351
116. Krämer C, Jaspers N, Nierhoff D, Kuhr K, Bowe A, Goeser T, et al. Acoustic structure quantification ultrasound software proves imprecise in assessing liver fibrosis or cirrhosis in parenchymal liver diseases. *Ultrasound Med Biol* 2014;40:2811-2818
117. Ho MC, Lee YH, Jeng YM, Chen CN, Chang KJ, Tsui PH. Relationship between ultrasound backscattered statistics and the concentration of fatty droplets in livers: an animal study. *PLoS One* 2013;8:e63543
118. Wan YL, Tai DI, Ma HY, Chiang BH, Chen CK, Tsui PH. Effects of fatty infiltration in human livers on the backscattered statistics of ultrasound imaging. *Proc Inst Mech Eng H* 2015;229:419-428
119. Tang A, Desai A, Hamilton G, Wolfson T, Gamst A, Lam J, et al. Accuracy of MR imaging-estimated proton density fat fraction for classification of dichotomized histologic steatosis grades in nonalcoholic fatty liver disease. *Radiology* 2015;274:416-425

https://doi.org/10.3348/kjr.2021.0112

120. Linares I, Hamar M, Selzner N, Selzner M. Steatosis in liver transplantation: current limitations and future strategies. *Transplantation* 2019;103:78-90
121. Veteläinen R, van Vliet A, Gouma DJ, van Gulik TM. Steatosis as a risk factor in liver surgery. *Ann Surg* 2007;245:20-30
122. Kleiner DE, Brunt EM, Van Natta M, Behling C, Contos MJ, Cummings OW, et al. Design and validation of a histological scoring system for nonalcoholic fatty liver disease. *Hepatology* 2005;41:1313-1321
123. Sandrin L, Fourquet B, Hasquenoph JM, Yon S, Fournier C, Mal F, et al. Transient elastography: a new noninvasive method for assessment of hepatic fibrosis. *Ultrasound Med Biol* 2003;29:1705-1713
124. Castera L, Forns X, Alberti A. Non-invasive evaluation of liver fibrosis using transient elastography. *J Hepatol* 2008;48:835-847
125. Friedrich-Rust M, Ong MF, Martens S, Sarrazin C, Bojunga J, Zeuzem S, et al. Performance of transient elastography for the staging of liver fibrosis: a meta-analysis. *Gastroenterology* 2008;134:960-974
126. Castera L, Friedrich-Rust M, Loomba R. Noninvasive assessment of liver disease in patients with nonalcoholic fatty liver disease. *Gastroenterology* 2019;156:1264-1281.e4
127. Joo I, Kim SY, Park HS, Lee ES, Kang HJ, Lee JM. Validation of a new point shear-wave elastography method for noninvasive assessment of liver fibrosis: a prospective multicenter study. *Korean J Radiol* 2019;20:1527-1535
128. Lee DH, Lee JY, Bae JS, Yi NJ, Lee KW, Suh KS, et al. Shear-wave dispersion slope from US shear-wave elastography: detection of allograft damage after liver transplantation. *Radiology* 2019;293:327-333
129. Sugimoto K, Moriyasu F, Oshiro H, Yoshimasu Y, Takeuchi H, Kasai Y, et al. Value of viscosity and viscoelasticity measurement in patients with NAFLD using shear wave ultrasound elastography. *Kanzo* 2018;59:370-373

 https://doi.org/10.3348/kjr.2021.0112